Complex magnetic transitions and possible orbital ordering in multiferroic Co_3TeO_6 single crystal

C. B. Liu,[1,2] C. C. Ma,[1] T. Li,[2] H. W. Wang,[2] R. Chen,[3] M. Y. Cui,[4] J. B. Cheng,[1] J. B. He,[1] S. J. Jin,[1] Y. S. Luo,[1,3,*] and J. F. Wang[2,†]

[1]*Henan International Joint Laboratory of MXene Materials Microstructure, College of Physics and Electronic Engineering, Nanyang Normal University, Nanyang 473061, People's Republic of China*

[2]*Wuhan National High Magnetic Field Center and School of Physics, Huazhong University of Science and Technology, Wuhan 430074, China*

[3]*Key Laboratory of Microelectronics and Energy of Henan Province, Henan Joint International Research Laboratory of New Energy Storage Technology, Xinyang Normal University, Xinyang 464000, People's Republic of China*

[4]*State Key Laboratory of Structural Chemistry, Fujian Institute of Research on the Structure of Matter, Chinese Academy of Sciences, Fuzhou, Fujian 350002, China*

(Received 17 December 2023; accepted 7 May 2024; published 4 June 2024)

Multiferroic material Co_3TeO_6 exhibits a sequence of structural and magnetic phase transitions, reflecting the interplay of lattice, orbit, and spin degrees of freedom. Here we report a different avenue to single-crystal growth and related morphology of Co_3TeO_6, and the compound is studied by magnetic susceptibility, specific heat, high-field magnetization, and electric polarization. We find that both magnetic susceptibility and specific heat in Co_3TeO_6 develop antiferromagnetic ordering ~26 K and a first-order phase transition ~18 K. The emergence of an increase of magnetic moment in magnetic susceptibility is compatible with the anomaly in specific heat for $H \| b$—we suppose that is ascribed to the orbital physics because of the degenerate state of t_{2g} in Co^{2+} ions. Low-field magnetization shows complex magnetic transitions and strong anisotropy in the system. Two spin flop transitions have been observed in high-field magnetization curve when magnetic field up to 55 T is applied along the b axis. The changes of electric polarization are compatible with the magnetic transitions in magnetization. Those results reveal that the complex transitions arise from the competing interactions among spin, lattice, orbit, and external magnetic field.

DOI: 10.1103/PhysRevB.109.214408

I. INTRODUCTION

The coupling between ferroelectric and magnetic order in multiferroic material has been attracting much attention owing to the feature of coexistence of them [1–4]. In special materials a strong interplay is found between electric polarization and noncollinear magnetic order. The mechanism of the polarization is associated with the spiral spin-driven ferroelectricity originating from vector spin chirality that breaks space-inversion symmetry [5,6]. In particular, a group of multiferroics such as $RMnO_3$ [7], $Ni_3V_2O_8$ [8], $LiCoPO_4$ [9], and $GdMn_2O_5$ [10] exhibits that the induction of polarization can be significantly affected by the application of a magnetic field. Those are possibly due to the fragile long-wavelength magnetic structure of the frustrated magnetic system [11]. In frustrated magnets, the inability of spins to satisfy the conflicting interactions results in a large degeneracy of the ground state at the classical level. Magnets of this kind have rather unusual properties. Here, we study another frustrated antiferromagnet material Co_3TeO_6, which shows coupling between ferroelectricity and magnetic structure [12]. Our goal is to present the growth and field-induced phase transition in the compound.

So far, Hudl *et al.* reported the study of the magnetic phase of a prototypical multiferroic material Co_3TeO_6 [12]. Co_3TeO_6 is crystallized in monoclinic space group $C2/c$ at room temperature with $\beta = 94.8^\circ$, as shown in Fig. 1(a). As β is rather close to 90°, the axis a can be replaced by the a^* in the measurement as shown in Fig. 1(a), where the a^* is perpendicular to the c axis. The crystal structure is characterized by layered arrangements, i.e., distorted zigzag chain and honeycomb web. Co^{2+} in each unit cell occupies five inequivalent sites, labeled as Co(1), Co(2), Co(3), Co(4), and Co(5), respectively. All the Co^{2+} are surrounded by the oxygen atoms, forming tetrahedron and octahedron. Except for the $Co(5)O_4$ tetrahedron, the other sites of Co ions include six oxygen constructing octahedrons. Ivanov and Li report that spins of Co^{2+} develop short- and long-range antiferromagnetic ordering, giving rise to complex magnetic transitions [13,14]. Those complex magnetic structures refer to the electric polarization triggered by magnetic fields, like frustrated antiferromagnet $Ni_3V_2O_8$ [15] and $Fe_2(MoO_4)_3$ [16]. As a consequence, the symmetry of the lattice is expected to be broken by spins, resulting in the electric polarization driven by magnetic field. In fact, Co_3TeO_6 is an excellent candidate material to study the electric polarization modulated by the magnetic field [12]. However, the research on Co_3TeO_6 involved magnetic and ferroelectric material remains unexplored in the last decade, as well as the field-induced magnetic phases of the b axis. One main reason is most likely the fact that Co_3TeO_6 single crystal is merely grown by the chemical vapor phase method with

*ysluo@xynu.edu.cn
†jfwang@hust.edu.cn

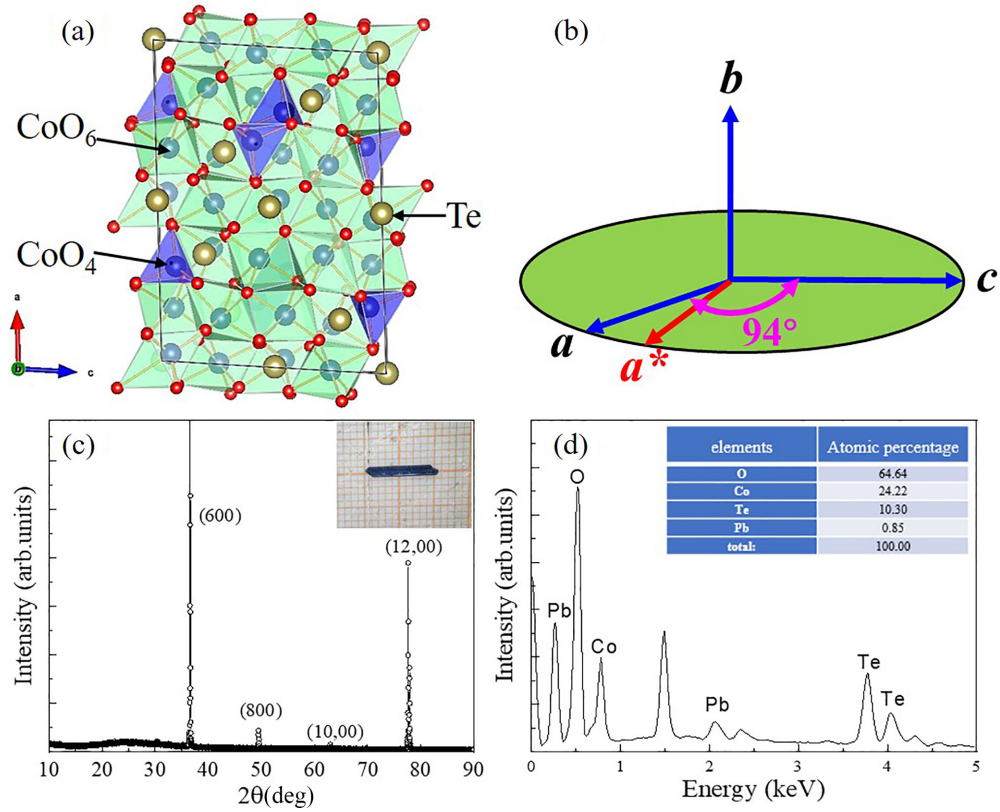

FIG. 1. (a) Crystal structure of Co_3TeO_6 viewed along the b axis, the octahedra and tetrahedra present CoO_6 and CoO_4, respectively. Te atoms (light brown) are separated by the oxygen polyhedron. (b) Respective schematic orientations of crystallographic axes, where the a^* is perpendicular to the b axis. (c) X-ray diffraction pattern on the natural surface of Co_3TeO_6 single crystal. Inset: the image of the as-grown single crystal with the largest sizes. (d) The EDS data mapping from the surface of single crystal.

transporting agent $PtCl_2$ or HCl [12,17], which hinders the measurements performed to explore the relationship between magnetism and ferroelectric. Here, we provide an alternative way to obtain Co_3TeO_6 single crystal and study its magnetic properties. We provide high-field-magnetization measurements of Co_3TeO_6 at various temperatures. We find the relevance between the sharp change of magnetic moment and the anomaly in specific heat. Those results infer that the first-order phase transition may be attributed to the orbital physics.

II. EXPERIMENT

Single crystals of Co_3TeO_6 were grown by the flux method, the synthesis of which was purely accidental. Stoichiometric amount of PbO (99%), $CoC_2O_4 \cdot 2H_2O$ (99%), and TeO_2 (99.99%) were ground with a molar ratio of 1:1:2 in an agate mortar and then sintered in air at 700 °C for 20 h. The reactant was compressed into a plate and fired at 450 °C for 20 h, and the process was repeated one more time. Then the product was mixed with flux $PbCl_2$ (99.99%) with a molar ratio of 1:1 in a platinum crucible, and heated to 850 °C. The melt liquid was cooled down to 650 °C at the rate of 2 °C/h, and the final product was determined to be crystal Co_3TeO_6 without element Pb. Obtained crystals were checked by powder x-ray diffraction; one natural surface of the crystal was determined to be the bc plane as is shown in Fig. 1(c). A single crystal of Co_3TeO_6 with a maximum size is up to $10 \times 1.5 \times 0.5\,mm^3$, as shown in the inset. The primary elements in the compound examined by energy dispersive spectrometer (EDS) were confirmed to be Co, Te, and O with a small amount of Pb, as shown in Fig. 1(c). The molar ratio of Co and Te was measured to be approximately 3:1. The temperature and low magnetic field dependence of magnetization were measured by using a commercial SQUID (superconducting quantum interference device) magnetometer. High-field magnetization and electric polarization measurements were extended to 55 T in a long pulse magnet at Wuhan National High Magnetic Field Center (WHMFC), China. The absolute value of magnetic moment in pulsed field was calibrated by that measured at static field. The value of electric polarization P_a was obtained by integrating the zero-electric-field pyroelectric current. Before each measurement of P_a, a bias electric field of $E = 500\,kV/m$ was applied to the sample. Specific-heat measurements were performed between 2 and 100 K using a Quantum Design physical property measuring system by the relaxation method.

III. RESULTS AND DISCUSSION

A. Low-field magnetization

Figure 2 shows the magnetic susceptibility $[\chi(T)]$ of single crystal of Co_3TeO_6 measured at $H = 0.1$ T for three axes. The large difference among the three axes $\chi(T)$ reflects strong anisotropy because of the anisotropic g factor and exchange interaction. A broad peak (T_{p1}) is observed around 30 K for $H \| c$, implying the development of antiferromagnetic order-

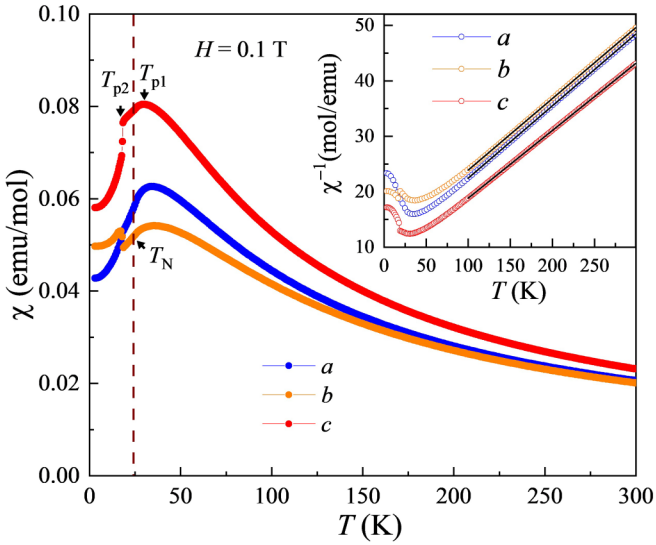

FIG. 2. Magnetic susceptibility $\chi(T)$ for each axis as a function of temperature in $H = 0.1$ T. The peaks associated with two transitions (labeled by T_{p1} and T_{p2}) are shown by downward arrows, and the dashed line indicates the long-range antiferromagnetic ordering. The inset shows the inverse susceptibility $1/\chi$ as a function of temperature, and the solid line is the Curie-Weiss fit with equation.

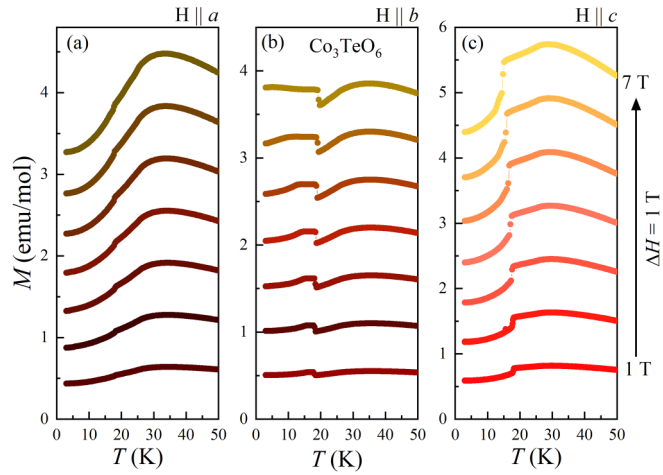

FIG. 3. Magnetization in Co_3TeO_6 measured at different various magnetic fields for crystallographic axes (a) $H\|a$, (b) $H\|b$, and (c) $H\|c$.

ing. An abrupt drop (T_{p2}) is exhibited at 18 K, suggesting the existence of the other magnetic order. For $H\|a$, the broad peak is shifted to ~34 K and accompanied by an inflection point at $T_{p2} \sim 18$ K. Those results are in agreement with the previous works [12,14], showing complex magnetic transitions and strong anisotropy, as well as demonstrating that the as-grown crystal is Co_3TeO_6. In addition to $\chi(T)$ curves recorded on the a and c axes, the magnetic properties were measured by applying magnetic fields along the b axis. Analogous to that observed in $H\|a$, $\chi(T)$ shows a broad peak at T_{p1}. Note that there is a sudden increase of and gradual reduction of $\chi(T)$ when the magnetic field is applied along the b axis. This would reflect the fact that an additional magnetic transition along the b axis arises at T_{p1}. According to the Curie-Weiss law,

$$\frac{1}{\chi} = \frac{T - \Theta_{CW}}{C},$$

the high-temperature $\chi(T)$ curve is fitted, where Θ_{CW} is the paramagnetic Curie temperature and C is the Curie-Weiss constant, respectively. The fitting above 100 K is exhibited in the inset in Fig. 2. By using the equation, the obtained parameters' effective magnetic moment μ_{eff} and Θ_{CW} are $\mu_{eff} = 4.5\mu_B$, $\Theta_{CW} = -72.4$ K for $H\|a$, $\mu_{eff} = 4.55\mu_B$, $\Theta_{CW} = -85.6$ K for $H\|b$, $\mu_{eff} = 4.68\mu_B$, $\Theta_{CW} = -54.8$ K for $H\|c$. The calculated effective magnetic moments are all greater than the spin-only value of $3.88\mu_B$ ($g = 2$) for $S = 3/2$ of Co^{2+}. The negative constants indicate the antiferromagnetic nature of exchange interaction between Co^{2+} spins. Considering antiferromagnetic ordering at $T_N = 26$ K, the frustrated factors are estimated to be ~3. This indicates that Co_3TeO_6 is a frustratedlike spin system with antiferromagnetic interactions.

In order to reveal the magnetic transitions of Co_3TeO_6, the evolution of magnetization M as a function of temperature T influenced by the magnetic field is presented in Fig. 3. For $H\|a$, $\chi(T)$ exhibits a rounded maximum at $T_{p1} = 34$ K and a small cusp at $T_{p2} = 18$ K because of antiferromagnetic interactions. With increasing field, the maximum peak and transition temperature T_N do not move significantly while the peak becomes distinct. For $H\|c$, it is observed that the broad peak $T_{p1} = 30$ K is almost independent to magnetic field, while the slope of magnetization below T_{p2} is changed once magnetic field is enhanced. This implies that magnetic field induces the change of magnetic structure of antiferromagnetic state. With respect to $H\|b$, the broad peak is remarkable since as the field increases, the magnitude of magnetic moment is enlarged as well. The evolution of magnetic moment suggests that spin-lattice coupling leads to a consequence of phase transition involving a change of magnetic moment.

In Fig. 4, we present the feature in dM/dT at various magnetic fields for three orientations to explore the magnetic transitions in details [14]. It is clear seen that the antiferromagnetic order T_N and the sharp peaks T_{p2} in three directions almost remain unchanged. Apart from that the observation of two transitions, the evolutional M (T) affected by magnetic field reveals several distinct peaks, marked by different symbols. The peaks are shifted toward to same direction as the field increases for $H\|a$ and $H\|b$, while no additional peak is observed in $H\|c$ except the peaks at T_{p2} and T_N. Those results demonstrate that complex magnetic transitions are triggered by magnetic fields in Co_3TeO_6, in agreement with earlier works. In addition, it is uncertain that whether the anomalies in the dashed ellipse region are ascribed to the magnetic transitions.

B. Specific heat

Figure 5 shows the specific heat C_p as a function of temperature with $H = 0$ T. There is a pronounced hump at around 26.5 K and a very sharp peak anomaly near 18 K, consistent with the magnetic transition in $\chi(T)$. The small peak is ascribed to the presence of antiferromagnetic ordering of spins, while the sharp one is attributed to a reconstructive first-order phase transition. Note that the contributions

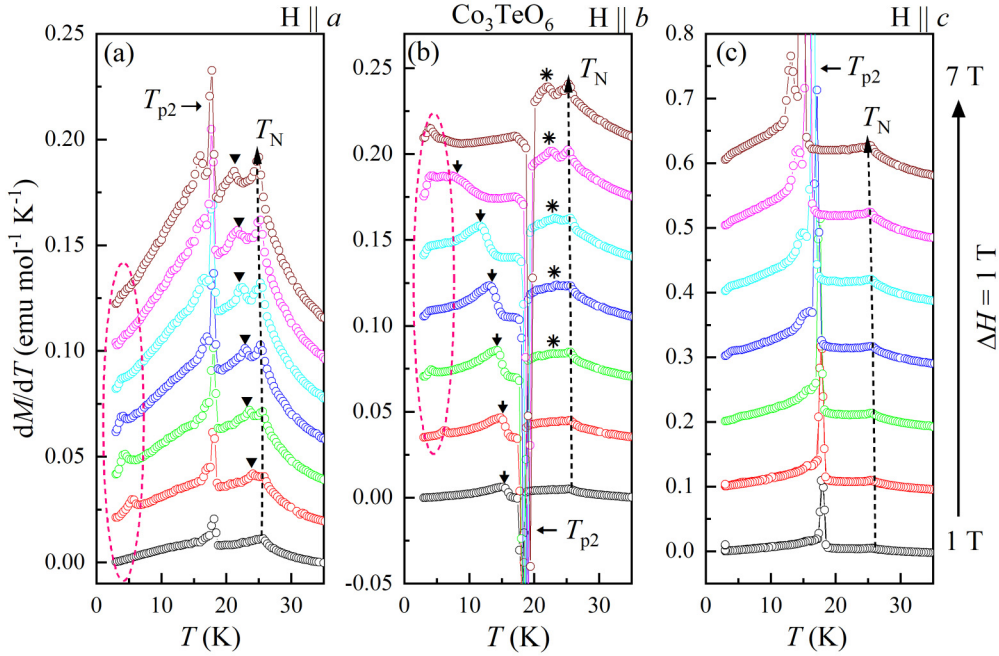

FIG. 4. The derivative of magnetization (M) with respect to temperature (T) at various magnetic fields from 1 to 7 T. The symbols indicate the anomaly induced by the magnetic field, suggesting magnetic transitions.

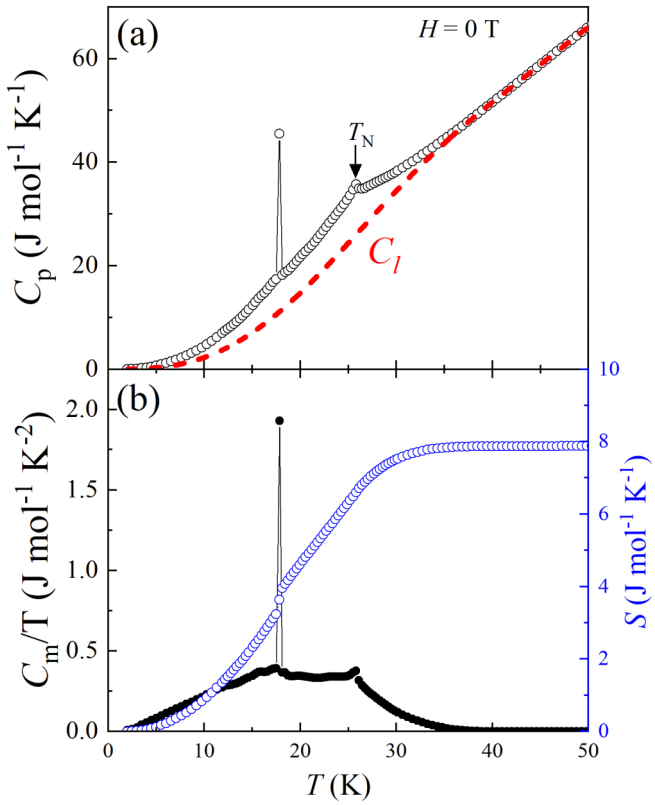

FIG. 5. (a) Specific heat C_p of Co_3TeO_6 as a function of temperature. The red solid line corresponds to the lattice specific heat C_l estimated from the expression $C_l = \beta_1 T^3 + \beta_2 T^5 + \beta_3 T^7$. (b) The magnetic specific heat and corresponding magnetic entropy.

of specific heat are composed of a magnetic part (C_m) and lattice (C_l). Therefore, the magnetic specific heat C_m is derived from subtracting lattice contribution C_l from the total specific heat C_p as is shown in Fig. 5(a). The magnetic entropy S_{mag} is estimated by integrating the C_m/T data, yielding a change of entropy $S_{mag} \sim 7.87$ J (mol K), as shown in Fig. 5(b). Considering that the spin of Co^{2+} is identified as $S = 3/2$ [18], the value of magnetic entropy reaches the percentage of 22.8% relevant to the standard estimation $S_{mag} = nR\ln(2S + 1) = 34.56$ J (mol K), where R is the universal gas constant and the n is the number of magnetic ions in the unit cell. The reduction of magnetic entropy indicates that the ground state of Co_3TeO_6 is preferred to be a noncollinear magnetic structure instead of antiferromagnetic ordering in three dimensions.

C. High-field magnetization

Given the fact that the magnetization curves of Co_3TeO_6 are introduced for $H \| a$ and $H \| c$ in the literature [14], here we only present the magnetization data of the compound with respect to $H \| b$. Figure 6 shows the magnetization along the b axis of Co_3TeO_6 in pulsed field up to 55 T at two selected temperatures 4.2 and 7 K. At 4.2 K, magnetization quasilinearly increases and two small kinks involved in magnetic transitions are individually observed at $H_{c1} \sim 5.6$ T and $H_{c2} \sim 35$ T, as shown in Fig. 6(a). The transitions are remarkably evidenced by the derivative dM/dH as a function of magnetic field. When the magnetic field is increased at 7 K, the process of magnetization remains unchanged and accompanies two kinks. The variation trend of magnetization curve is similar to that observed in $H \| a$ and $H \| c$, of which the transitions have

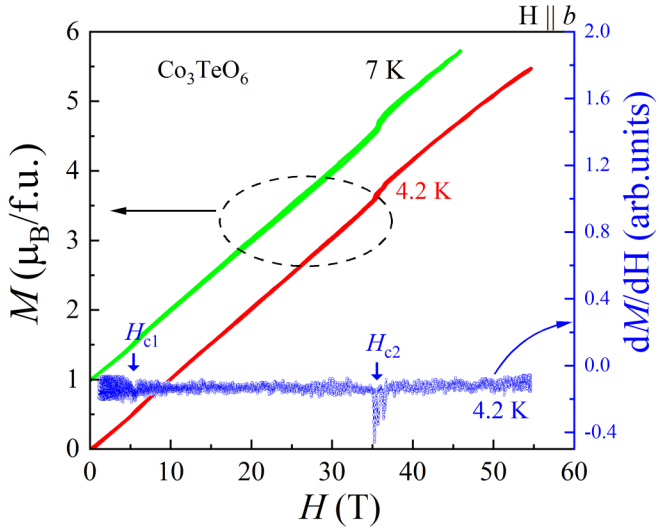

FIG. 6. Raw magnetization curve of Co_3TeO_6 single crystal measured at two temperatures and the derivative dM/dH of magnetization vs magnetic field H for $T = 4.2$ K. The H_{c1} and H_{c2} denote the critical fields of spin-flop transition. For clarity, the data measured at two temperatures are offset along the vertical axis.

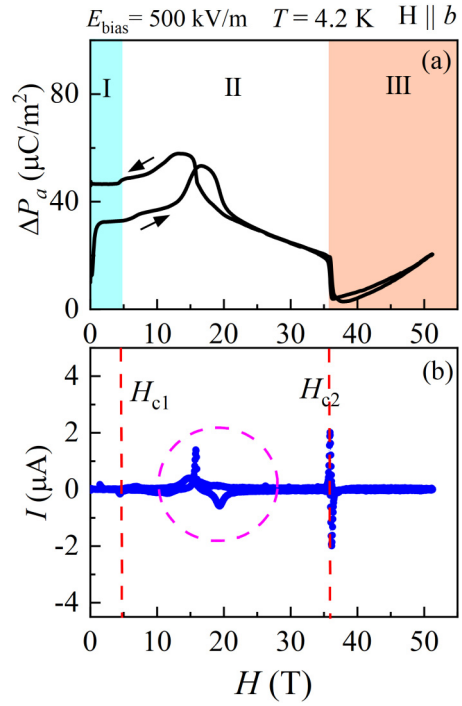

FIG. 7. The electric polarization (a) and corresponding pyroelectric current (b) of Co_3TeO_6 measured at 4.2 K for $P\|a$, $H\|b$. The sample was cooled down under a poling electric field of 500 kV/m. Phases I, II, and III are ferroelectric states, H_{c1} and H_{c2} are critical fields of magnetic transition and pyroelectric current. The dashed circle denotes the change of the pyroelectric current.

been discussed originating from the magnetic field induced spin flop transition [14]. Hence, the magnetic transitions for $H\|b$ are very likely the antiferromagnetic interaction suppressed by the field, giving rise to the establishment of new spin flop transitions. Moreover, the expected magnetic moment is calculated to be $1.8\mu_B/Co^{2+}$ with field $H \sim 55$ T, which is much less than the expected saturation magnetization $3\mu_B/Co^{2+}$ (considering spin only). In addition, no magnetic hysteresis is visible between the ascending- and descending-field process.

D. High-field electric polarization

In order to determine the magnetic transitions, we further investigate the electric polarization of Co_3TeO_6 in a pulse field up to 52 T. Only P_a can be achieved because only one large crystalline plane bc can be determined. Figure 7 shows the field dependence of electric polarization P_a and corresponding pyroelectric current I measured at 4.2 K. Nonzero polarization is observed through the whole field sweep process when magnetic field is applied for $H\|b$, as is shown in Fig. 7(a). Taking into account the fact that two changes in P_a are individually observed at $H_{c1} \sim 5$ T and $H_{c2} \sim 35$ T, the polarization curve can be separated into three phases, I, II, and III. Possible spontaneous polarization P_a in phase I is measured [12]; we therefore suppose that the polarized states II and III can be classified as another two ferroelectric phases. The boundaries of the states are in agreement with the magnetic transitions detected in magnetization, which is remarkably evidenced by the peaks in pyroelectric current [see Fig. 7(b)]. The results indicate that the emergence of electric polarization is strongly dependent on the magnetic orders. However, the large ferroelectric phase and pyroelectric current in phase II show no correlation with the magnetic transitions, indicative of more complex polarization behavior in Co_3TeO_6 under external magnetic field, like magnetic-driven multiferroic $MnWO_4$ [19] and $Co_4Nb_2O_9$ [20]. More experiments are desired to study the magnetic transitions and polarization with application of magnetic field.

E. Discussion

According to the symmetry analysis, the lattice parameters a, b, and c in monoclinic structure $C2/c$ are usually found to be different. The common feature of the structure is anisotropic; typical materials are such as α-CoV_2O_6 [21], applying equally to Co_3TeO_6. Successive spin flop phase transitions and ferroelectric response are reported in the presence of magnetic field in both $H\|a$ and $H\|c$; a spiral magnetic structure is proposed to explain the origin of the polarization. In this case, the two spin flop transitions in $H\|b$ induced by the magnetic field are the most favorable to describe the change of magnetic structure of Co_3TeO_6. Combined with the results described in the literature [14], multistep spin flop transitions are demonstrated by high-field magnetization, suggesting that the ground state of Co_3TeO_6 is not solely adopted for the antiparallel spin state. One possibility of a spin state has been classified as a superantiferromagnetic phase to explain the complex magnetic transition [14], due to the fact that low field magnetic order of state I is an incommensurate phase, giving rise to the ferroelectric phase I. Moreover, no saturated state can be achieved at $\boldsymbol{H} \sim 52$ T, indicating that phase II is a spin unpolarized state. Therefore, the magnetic orders of state II and III are supposed to be a spiral state instead of an ordering

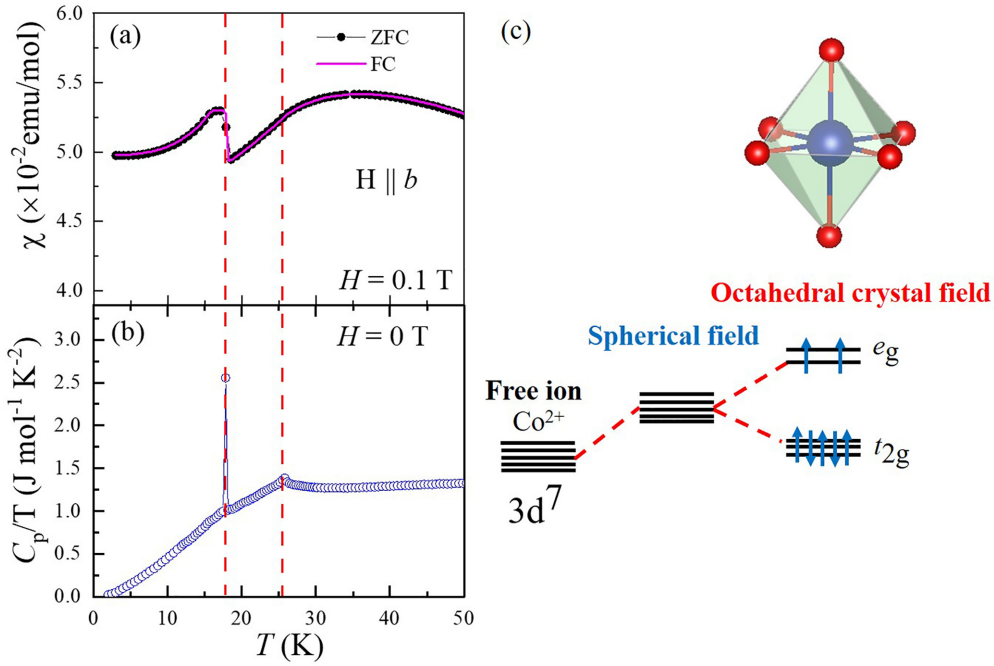

FIG. 8. (a) Magnetic susceptibility for $H \| b$ and (b) zero field specific heat. (c) Schematic sketch of the energy level split of Co^{2+} in octahedra due to the spherical field and the octahedral crystal field.

state, by which we can explain the ferroelectric polarization originating from the magnetic order with a spin current model or Dzyaloshinsky-Moriya interaction.

On the other hand, one promising feature of Co_3TeO_6 is the observation of the first-order phase transition behavior. As shown in Figs. 8(a) and 8(b), one can see that the abnormal signature of magnetic moment is compatible with a sharp peak in specific heat. This implies that the two features have one common origin. Notably, no difference is observed between zero-field-cooled (ZFC) and FC curves, excluding ferromagnetic interaction for the increase of magnetic moment. We propose two alternative theories which are combined with the structural data and nontrivial magnetic behavior for $H \| b$. In one model, the anomaly of magnetic moment seemingly arises from orbit physics, including the interplay of spin-orbit and spin-lattice couplings [14]. The magnetism of the compound is governed by Co^{2+} and Co^{3+} ions, and it has been stated that the structure of Co_3TeO_6 can be regarded as an analog of spinel compound $Co^{2+}Co_2^{3+}O_4$ [14,18,22]. In this case, we find several common characteristics between Co_3TeO_6 and vanadium spinels AV_2O_4 (A = Zn, Cd) [23], which are expected to explore the orbit physics [24,25]. In AV_2O_4, the two d electrons of V^{3+} have spin $S = 1$ and occupy two out of three t_{2g} orbitals. The ordered orbital state is preferred to be antiferro-orbital and ferro-orbital ordering in ZnV_2O_4 [25] and CdV_2O_4 [26]. Since Co^{2+} ions in an octahedra environment have orbital degree of freedom ($S = 3/2$, $\tilde{l} = 1$) [27,28], the magnetic moments are not classified as nearly ideal Heisenberg spins system. The common features between two systems mainly contain three aspects: (1) sudden change of magnetic susceptibility and discontinuity anomaly in specific heat [23]; (2) the orbital states of magnetic ions V^{3+} (t_{2g}^2) and Co^{2+} ($e_g^2 t_{2g}^5$) ions are degenerate—the splits of orbital states of Co^{2+} because of the crystal-field effect in octahedral structure are illustrated in Fig. 8(c); (3) the structure of Co_3TeO_6 is similar to the spinel compound. Therefore, we conclude that the anomaly of the magnetic moment for $H \| b$ is ascribed to the degeneration of the orbital state of Co ions. The lattice is strongly coupled to the orbit degrees of freedom, giving rise to the distortion of the oxygen polyhedron [26]. Hence, the collective distortion of lattice along the b axis is the cause of the first-order phase transition in specific heat, involving the spin-orbit and spin-lattice couplings. Note that the presence of orbital degree of freedom may change the physics of degeneracy lifting [26]. This is likely to be another origin for the complex magnetic transitions in Co_3TeO_6. The other model is supposed to be from the electronic charge redistribution of Co, giving rise to the structural distortion and change of magnetic moment [22]. This seems like the lattice distortion is stated in the charge density wave (CDW) system [29–32]. However, further adequate investigations by other experimental techniques are necessary to uncover the exact origin of first-order phase transition. In combination with previous results, those observations relevant to thermal and magnetism imply direct interplay between spin, lattice, and orbit degrees of freedom.

IV. CONCLUSION

To conclude, we have studied the crystal growth, magnetic susceptibility, specific heat, and high-field magnetization of Co_3TeO_6 single crystal. The flux method was first presented to be an alternative way to obtain Co_3TeO_6 single crystal. We have observed complex magnetic transitions in magnetic susceptibility as a function of temperature and magnetic field. Especially, the sudden change of magnetic moment for $H \| b$

is associated to the sharp anomaly in specific heat, revealing orbital physics in Co_3TeO_6. In addition, two distinct magnetic phase transitions compatible with two changes of electric polarization are observed when magnetic field is applied for $H \| b$. Our results confirm that Co_3TeO_6 is an anisotropic antiferromagnet with complex magnetic transitions at low temperatures. Another aspect that deserves attention in the present study is the existence of strong magnetic anisotropy in $H \| a$ and $H \| b$. More experiments should be further utilized to explore magnetic physics for applying a magnetic field along the b axis.

ACKNOWLEDGMENTS

We gratefully thank C. Dong, Y. Feng, and Z. Wu for high-field magnetization, electric polarization, and specific-heat measurements. This work was supported by the National Natural Science Foundation of China (Grants No. 12104388, No. 12074135, No. 12104351, No.11404175, No. 52272219), the Natural Science Foundation of Henan Province of China (Grant No. 232300421220), the Hubei Province Natural Science Foundation of China (Grant No. 2021CFB027), and the China Postdoctoral Science Foundation (Grant No. 2023M731209).

[1] M. Mostovoy, Ferroelectricity in spiral magnets, Phys. Rev. Lett. **96**, 067601 (2006).
[2] Y. Yamasaki, H. Sagayama, T. Goto, M. Matsuura, K. Hirota, T. Arima, and Y. Tokura, Electric control of spin helicity in a magnetic ferroelectric, Phys. Rev. Lett. **98**, 147204 (2007).
[3] Y. Tokura, S. Seki, and N. Nagaosa, Multiferroics of spin origin, Rep. Prog. Phys. **77**, 076501(2014).
[4] E. Gradauskaite, P. Meisenheimer, M. Müller, J. Heron, and M. Trassin, Multiferroic heterostructures for spintronics, Phys. Sci. Rev. **6**, 2 (2021).
[5] H. Katsura, N. Nagaosa, and A. V. Balatsky, Spin current and magnetoelectric effect in noncollinear magnets, Phys. Rev. Lett. **95**, 057205 (2005).
[6] S. W. Cheong, D. Talbayev, V. Kiryukhin, and A. Saxena, Broken symmetries, non-reciprocity, and multiferroicity, Npj Quantum. Mater. **3**, 19 (2018).
[7] T. Kimura, G. Lawes, T. Goto, Y. Tokura, and A. P. Ramirez, Magnetoelectric phase diagrams of orthorhombic $RMnO_3$ (R = Gd, Tb, and Dy), Phys. Rev. B **71**, 224425 (2005).
[8] Y. J. Liu, J. F. Wang, Z. Z. He, C. L. Lu, Z. C. Xia, Z. W. Ouyang, C. B. Liu, R. Chen, A. Matsuo, Y. Kohama, K. Kindo, and M. Tokunaga, Unusual magnetoelectric memory and polarization reversal in the Kagome staircase compound $Ni_3V_2O_8$, Phys. Rev. B **97**, 174429 (2018).
[9] A. S. Zimmermann, D. Meier, and M. Fiebig, Ferroic nature of magnetic toroidal order, Nat. Commun. **5**, 4796 (2010).
[10] L. Ponet, S. Artyukhin, T. Kain, J. Wettstein, A. Pimenov, A. Shuvaev, X. Wang, S. W. Cheong, M. Mostovoy, and A. Pimenov, Topologically protected magnetoelectric switching in a multiferroic, Nature (London) **607**, 81 (2022).
[11] K. Taniguchi, N. Abe, T. Takenobu, Y. Iwasa, and T. Arima, Ferroelectric Polarization flop in a frustrated magnet $MnWO_4$ induced by a magnetic field, Phys. Rev. Lett. **97**, 097203 (2006).
[12] M. Hudl, R. Mathieu, S. A. Ivanov, M. Weil, V. Carolus, Th. Lottermoser, M. Fiebig, Y. Tokunaga, Y. Taguchi, Y. Tokura, and P. Nordblad, Complex magnetism and magnetic-field-driven electrical polarization of Co_3TeO_6, Phys. Rev. B **84**, 180404(R) (2011).
[13] S. A. Ivanov, R. Tellgren, C. Ritter, P. Nordblad, R. Mathieu, G. André, N. V. Golubko, E. D. Politova, and M. Weil, Temperature-dependent multi-k magnetic structure in multiferroic Co_3TeO_6, Mater. Res. Bull. **47**, 63 (2012).
[14] J. L. Her, C. C. Chou, Y. H. Matsuda, K. Kindo, H. Berger, K. F. Tseng, C. W. Wang, W. H. Li, and H. D. Yang, Magnetic phase diagram of the antiferromagnetic cobalt tellurate Co_3TeO_6, Phys. Rev. B **84**, 235123 (2011).
[15] C. Dong, J. F. Wang, Z. Z. He, Y. T. Chang, M. Y. Shi, Y. R. Song, S. M. Jin, Y. Q. Du, Z. Y. Wu, X. T. Han, K. Kindo, and M. Yang, Reentrant ferroelectric phase induced by a tilting high magnetic field in $Ni_3V_2O_8$, Phys. Rev. B **105**, 024427 (2022).
[16] A. Tiwari, D. C. Kakarla, M. J. Hsieh, J. Y Lin, C. W. Wang, L. K. Tseng, C. E. Lu, A. Pal, T. W. Kuo, M. Mitch. C. Chou, and H. D. Yang, Observation of magnetic field-induced second magnetic ordering and peculiar ferroelectric polarization in L-type ferrimagnetic $Fe_2(MoO_4)_3$, Phys. Rev. Mater. **6**, 094412 (2022).
[17] R. Becker, M. Johnsson, and H. Berger, A new synthetic cobalt tellurate: Co_3TeO_6, Acta Crystallogr. **C62**, i67 (2006).
[18] H. Singh, H. Ghosh, T. V. C. Rao, A. K. Sinha, and P. Rajput, Observation of high-spin mixed oxidation state of cobalt in ceramic Co_3TeO_6, J. Appl. Phys. **116**, 214106 (2014).
[19] J. F. Wang, W. X. Liu, Z. Z. He, C. B. Liu, M. Tokunaga, M. Li, C. Dong, X. T. Han, F. Herlach, C. L. Lu, Z. W. Ouyang, Z. C. Xia, K. Kindo, L. Li, and M. Yang, Ferroelectric polarization reversal in multiferroic $MnWO_4$ via a rotating magnetic field up to 52 T, Phys. Rev. B **104**, 014415 (2021).
[20] Y. T. Chang, J. F. Wang, W. Wang, C. B. Liu, B. You, M. F. Liu, S. H. Zheng, M. Y. Shi, C. L. Lu, and J. M. Liu, Linear magnetoelectric memory and training effect in the honeycomb antiferromagnet $Co_4Nb_2O_9$, Phys. Rev. B **107**, 014412 (2023).
[21] Z. Z. He, J. I. Yamaura, Yutaka Ueda, and W. D. Cheng, CoV_2O_6 Single crystals grown in a closed crucible: unusual magnetic behaviors with large anisotropy and 1/3 magnetization plateau, J. Am. Chem. Soc. **131**, 7554 (2009).
[22] C. H. Lee, E. Batsaikhan, M. H. Ma, W. H. Li, C. W. Wang, C. M. Wu, H. D. Yang, J. W. Lynn, and H. Berger, Charge transfer enhanced magnetic correlations in type-II multiferroic Co_3TeO_6, J. Chin. Chem. Soc. **68**, 395 (2020).
[23] A. N. Vasiliev, M. M. Markina a, M. Isobe b, and Y. Ueda, Specific heat and magnetic susceptibility of spinel compounds CdV_2O_4, ZnV_2O_4 and $MgTi_2O_4$, J. Magn. Magn. Mater. **300**, e375 (2006).
[24] S. Di Matteo, G. Jackeli, and N. B. Perkins, Orbital order in vanadium spinels, Phys. Rev. B **72**, 020408(R) (2005).
[25] S. H. Lee, D. Louca, H. Ueda, S. Park, T. J. Sato, M. Isobe, Y. Ueda, S. Rosenkranz, P. Zschack, J. Iniguez, Y. Qiu, and R. Osborn, Orbital and spin chains in ZnV_2O_4, Phys. Rev. Lett. **93**, 156407 (2004).

[26] C. Lacroix, P. Mendels, and F. Mila, *Introduction to Frustrated Magnetism: Materials, Experiments, Theory* (Springer, New York, 2011), Vol. 164, p. 166.

[27] T. Susuki, N. Kurita, Takuya Tanaka, H. Nojiri, A. Matsuo, K. Kindo, and H. Tanaka, Magnetization process and collective excitations in the $S = 1/2$ triangular-lattice heisenberg antiferromagnet $Ba_3CoSb_2O_9$, Phys. Rev. Lett. **110**, 267201 (2013).

[28] Y. Shirata, H. Tanaka, A. Matsuo, and K. Kindo, Experimental realization of a spin-1/2 triangular-lattice heisenberg antiferromagnet, Phys. Rev. Lett. **108**, 057205 (2012).

[29] T. Danz, T. Domrose, and C. Ropers, Ultrafast nanoimaging of the order parameter in a structural phase transition, Science **371**, 371 (2021).

[30] J. Z. Ke, M. Yang, H. P. Zhu, C. B. Liu, C. Dong, W. X. Liu, M. Y. Shi, and J. F. Wang, Reconstruction of the Fermi surface induced by high magnetic field in the quasi-two-dimensional charge density wave conductor η-Mo_4O_{11}, Phys. Rev. B **102**, 245135 (2020).

[31] X. F. Xu, A. F. Bangura, J. G. Analytis, J. D. Fletcher, M. M. J. French, N. Shannon, J. He, S. Zhang, D. Mandrus, R. Jin, and N. E. Hussey, Directional field-induced metallization of quasi-one-dimensional $Li_{0.9}Mo_6O_{17}$, Phys. Rev. Lett. **102**, 206602 (2009).

[32] R. E. Thorne, Charge-density-wave conductors, Phys. Today **49**(5), 42 (1996).